Pergamon

Int. J. Solids Structures Vol. 33, No. 12, pp. 1709–1723, 1996

0020–7683/96 $15.00 + .00

0020–7683(95)00119–0

NUMERICAL ANALYSIS OF THE INTERACTION OF SOLUTE HYDROGEN ATOMS WITH THE STRESS FIELD OF A CRACK

J. LUFRANO and P. SOFRONIS*

Department of Theoretical and Applied Mechanics, University of Illinois at Urbana-Champaign, 216 Talbot Laboratory, 104 South Wright Street, Urbana, IL 61801, U.S.A.

(*Received* 11 *October* 1994; *in revised form* 18 *May* 1995)

Abstract—Finite element analysis is used to study the effect of mobile interstitial hydrogen on the deformation of metals and alloys in the case when hydrogen is in equilibrium with local stresses. The effect is studied by calculating the hydrogen atmosphere around a stationary crack tip in a linearly elastic isotropic material loaded in mode I plane strain conditions. Stresses, strains and equilibrium hydrogen concentrations are determined through an iterative finite element analysis while accounting for stress relaxation due to hydrogen induced local volume and elastic modulus changes. Numerical calculations reveal a zone immediately ahead of the crack tip in which the lattice is saturated with hydrogen. The dimensionless size of the saturation zone is found to be independent of the applied loads. The stiffness derivative method is used to calculate the hydrogen induced changes in the stress intensity factor. Calculations show that the presence of mobile interstitial hydrogen produces crack tip shielding when hydrogen induced changes in the elastic moduli are considered. The implications of the elastic analysis of the interaction between hydrogen in equilibrium with local stresses near a crack tip on the fracture resistance of materials are discussed. Then results are examined in conjunction with the elastic-plastic deformation at the tip.

INTRODUCTION

The effect of solute hydrogen on the fracture behavior of metals and alloys has been widely investigated during the past 25 years. A recent review of studies and viable mechanisms of hydrogen embrittlement can be found in the work by Birnbaum and Sofronis (1994). Despite the intense research on the subject, a complete mechanistic understanding of the hydrogen embrittlement phenomena has yet to be achieved. While many mechanisms have been suggested, it appears certain that no single mechanism can account for all the complex behavior of metals in the presence of hydrogen. In any theory of hydrogen embrittlement, knowledge of the interaction between the elastic stress field of a crack tip and the associated hydrogen atmosphere is clearly of interest. The interaction between solute hydrogen and an applied stress field results from the hydrogen induced volume (Peisl, 1978) and local moduli changes (Mazzolai and Birnbaum, 1985a, 1985b) that accompany the introduction of the solute hydrogen in the lattice. The hydrogen volumetric and modulus effect on the elastic deformation of the material can then be analyzed by modeling (Sofronis and Birnbaum, 1995) the solutes as stress centers associated with a dilatational transformation strain (Eshelby, 1956, 1957) whose magnitude depends on the local hydrogen concentration.

The calculation of the solute hydrogen distribution at a crack tip in an isotropic linearly elastic solid was carried out by Van Leeuwen (1974) and Hippsley and Briant (1985) under non-steady state conditions of hydrogen transport. Calculations of hydrogen atmospheres at a crack tip in equilibrium with local stresses were done by Liu (1970) in an isotropic linearly elastic material and by Tong-Yi *et al.* (1992a, 1992b) in single crystals of elastically anisotropic iron. One dimensional hydrogen transport at a crack tip and the associated crack propagation in an elastic material was studied by Unger (1989). Dutton *et al.* (1977) modeled the hydrogen assisted fracture in commercial Zr-2.5%Nb alloy by allowing for hydride precipitation in a steady state hydrogen diffusion treatment. Sofronis and McMeeking (1989) analyzed the coupled hydrogen transient diffusion and plastic straining in the area around a blunting crack tip allowing also for hydrogen trapping at microstructural

*Author to whom correspondence should be addressed.

defects. A common feature of these analyses is that they do not consider the effects of hydrogen volume or modulus change on the elastic deformation of the lattice. As a result, the stresses in the solid and the associated boundary and initial value problems for stress driven diffusion are treated as unaffected by the solute hydrogen. It should be noted here that high hydrogen concentrations, usually at the lattice saturation level, prevail in the vicinity of stress raisers such as a crack tip. As a consequence, the corresponding hydrogen induced dilatational strain is important in relaxing the local stresses. The mechanics of toughening due to transforming precipitates (McMeeking and Evans, 1982; Budiansky *et al.*, 1982) and interstitial impurities (Weertman and Hack, 1988) is now well understood. Therefore a similar analysis can be applied to determine the hydrogen induced changes in the local stress intensity factor at a crack tip. These calculations should be useful in developing a better understanding of the reduced fracture resistance of materials in the presence of hydrogen.

In this paper, continuum mechanics analysis is used to investigate the hydrogen distribution in equilibrium with local stresses in front of a stationary crack loaded in plane strain mode I conditions. Transient effects resulting from the solute diffusion towards the crack tip and dynamic effects on the solute atmosphere are not considered. Fast redistribution of solute hydrogen allows for hydrogen atmosphere equilibration with the far field hydrogen concentrations and as a result the calculation corresponds to a constant chemical potential for hydrogen. The material is considered linearly elastic and isotropic and its constitutive law accounts for the hydrogen induced local dilatational strain and elastic modulus change. The elastic boundary value problem for the deformation of the solid is formulated and solved by an iterative finite element method (Sofronis and Birnbaum, 1993). The corresponding local hydrogen concentrations are obtained directly from the local stresses. However idealized, the complete solution to this coupled problem has not yet been examined and may help to illuminate some basic trends within the hydrogen embrittlement process. It has been suggested recently (Sofronis and Birnbaum, 1995; Birnbaum and Sofronis, 1994) that hydrogen can diminish the local stress fields from dislocations and solutes that act as barriers to the dislocation motion. In connection with this idea, the possibility of crack tip shielding or anti-shielding by solute hydrogen is investigated.

CONSTITUTIVE RELATION

In this section the constitutive law used to model the material deformation and calculate the hydrogen distribution is described. The model assumes that hydrogen once adsorbed and absorbed by the material resides in normal interstitial lattice sites in a continuous distribution throughout the lattice. Thus a continuum description for the solid solution material can be formulated. In this purely elastic calculation, trapping of hydrogen at microstructural defects is not considered.

The hydrogen concentration c, measured in atoms of hydrogen per solvent atom, is given by

$$c = \beta\theta, \tag{1}$$

where θ denotes the occupancy of the available interstitial sites, i.e. the ratio of occupied sites to the total available and β denotes the number of interstitial sites per solvent atom. The parameter β is fixed for a given lattice. The first order elastic interaction energy (Cottrell, 1948; Eshelby, 1957) associated with a hydrogen atom introduced against a stress field, σ, can be modeled (Sofronis and Birnbaum, 1995) by

$$W_{int} = -\tfrac{1}{3}\sigma_{kk}\Delta v, \tag{2}$$

where Δv is the volume change per host metal lattice that is directly related to the partial molar volume of hydrogen $V_H = \Delta v N_A$ in solution, where N_A is Avogadro's number, and

the standard summation convention is used over repeated indices throughout. Since the effect of hydrogen is studied at a crack tip loaded in mode I conditions, it is reasonable to expect that the interaction of hydrogen with the crack tip stress field is dominated by the first order interaction as given by eqn (2) due to the isotropic distortion field of the hydrogen atom. Thus, to simplify the calculations, one can omit the second order interaction energy (Sofronis and Birnbaum, 1995) between the hydrogen solutes and the crack tip. Then the local hydrogen concentration c in equilibrium with the local stresses σ is calculated with use of eqn (2) through the Fermi-Dirac form (Hirth and Carnahan, 1978)

$$\frac{\theta}{1-\theta} = \frac{\theta_0}{1-\theta_0} \exp\left(-\frac{W_{int}}{kT}\right), \tag{3}$$

where θ_0 is the interstitial site occupancy of the remote unstressed lattice at nominal concentration c_0, T is the absolute temperature and k is Boltzmann's constant. In the numerical calculations, the ratio H/M was taken to have a maximum equal to 1 corresponding to $\beta = 6$ and $\theta = 1/6$ for the tetrahedral interstitial site occupancy typical of BCC systems.

The deviatoric stress strain relationship for the isotropic solid solution material is

$$\sigma'_{ij} = 2\mu\varepsilon'_{ij} \tag{4}$$

where σ' is the deviatoric part of the stress, ε' is the deviatoric part of the strain and μ is the shear modulus. It has been experimentally verified (Peisl, 1978) that the distortion of the lattice due to hydrogen is a purely dilatational strain

$$\varepsilon^H_{ij} = \tfrac{1}{3} e^H \delta_{ij}, \tag{5}$$

where e^H is the local lattice dilatation given by (Sofronis and Birnbaum, 1995)

$$e^H = c\frac{\Delta v}{\Omega}, \tag{6}$$

where Ω is the mean atomic volume of the host metal atom and δ_{ij} is the Kronecker delta. Thus the dilatant behavior of the solid solution lattice is represented by

$$\varepsilon_{kk} = \frac{\sigma_m}{B} + e^H, \tag{7}$$

where ε_{kk} denotes the total dilatation, σ_m is the hydrostatic stress equal to $\sigma_{kk}/3$, and B is the bulk modulus of the material. In the present paper the model material was taken to be niobium whose elastic behavior was assumed to be isotropic. The hydrogen effect on the shear and bulk moduli is described respectively by

$$\mu = -9.8c + 40.9 \tag{8}$$

and

$$B = 169.6 + 10.4c \tag{9}$$

in units of GPa, where c is the local hydrogen concentration measured in atoms of hydrogen per atom of niobium. Equations (8) and (9) represent the Voigt averages of the isotropic elastic moduli calculated from measurements of the cubic moduli C_{11}, C_{12} and C_{44} as functions of the hydrogen concentration (Mazzolai and Birnbaum, 1985a, 1985b). As will be seen, the effects of hydrogen on the local stress intensity factor at a crack tip are strongly

associated with the decrease of the shear modulus with increasing hydrogen concentration. Equations (1), (2) and (3) for the calculation of the hydrogen concentration and eqns (4), (6), (7), (8) and (9) for the stress-strain law demonstrate the coupling of the material elastic deformation with the hydrogen distribution.

BOUNDARY VALUE PROBLEM

The purpose is to calculate the stresses and deformations near the tip of a long crack in plane strain in the presence of hydrogen solute atoms. The body is loaded so that only mode I (tensile opening mode) stresses arise at the tip. The relaxed elastic stress field associated with the introduction of hydrogen into the lattice is calculated near the crack tip while the elastic moduli of the lattice are allowed to vary pointwise according to the local hydrogen concentration. Calculation of the hydrogen concentration, which is coupled to the local hydrostatic stress, is carried out simultaneously. Attention is focused on a small scale zone of hydrogen enriched material which is confined to a region very close to the crack tip whose size is negligible compared with any dimensions of the specimen. Due to the local hydrogen enrichment the hydrogen induced dilatation inside the zone is much larger that the corresponding dilatation outside the zone. As a consequence, the problem can be studied by following the boundary layer approach (Rice, 1968a, b), namely by imposing tractions on a circular boundary far from the tip in agreement with the standard singular linear elastic solution given by

$$\sigma_{ij} = \frac{K_A}{\sqrt{2\pi r}} f_{ij}(\theta), \tag{10}$$

where K_A is the mode I stress intensity due to applied loads, (r, θ) are polar coordinates measured from the crack tip and f_{ij} is a given function that can be found in the work by Irwin (1960).

The condition for a small scale zone of hydrogen enriched material in a finite medium can be achieved if the hydrogen induced dilatational strain does not affect the stress field in the regions of the material remote from the tip. Such a requirement can be enforced by choosing the circular boundary (see Fig. 1), where the external loads are applied, quite remote from the tip so that the applied stresses near the boundary do not raise the corresponding local hydrogen concentrations significantly above the nominal or stress-free hydrogen concentration c_0. Then, for small nominal concentrations, the associated dilatational strains due to solute hydrogen near the boundary are small in comparison to the elastic strains caused by the applied loads in the absence of hydrogen. As a result, the concept of a small scale zone of hydrogen induced dilatational strain arising from an area confined to the crack tip is a valid one.

The mechanical equilibrium in the plane can be stated by the principle of virtual work in the absence of body forces as

$$\int_A \sigma_{ij} \delta \varepsilon_{ij} \, \mathrm{d}A = \int_S T_i \delta u_i \, \mathrm{d}S, \tag{11}$$

where A is the area and S is the perimeter of the domain, T_i is the component of the traction applied on S and u_i is the component of the displacement in A. The symbol δ indicates an arbitrary virtual variation of the quantity it precedes. In addition the stresses are related to the strains by the constitutive law given by eqns (4) and (7). Since the local dilatational strain due to hydrogen is dependent on the local hydrogen concentration which in turn is dependent on the local hydrostatic stress, governing eqn (11) is non-linear. Also, the variability of the local elastic moduli as a function of local hydrogen populations makes the constitutive equations non-linear. Therefore the problem of calculating the stress field and the local distribution of hydrogen is coupled in a non-linear sense and the solution procedure involves iteration (Sofronis and Birnbaum, 1993). Solution to the boundary

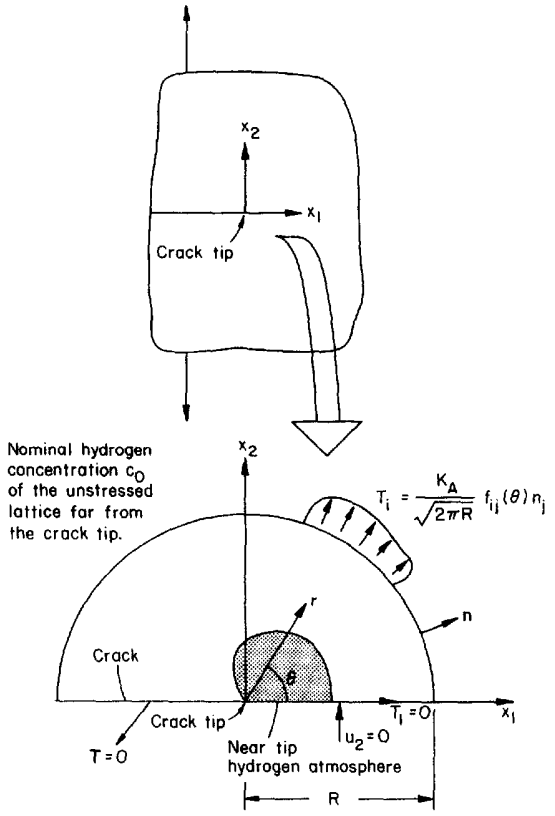

Fig. 1. The boundary value problem of a semi-infinite crack with its hydrogen atmosphere formed under mode I tensile opening load.

value problem is sought on the basis that the interactions between elastic stress centers are fast, thus allowing for local rearrangement of the solutes without changing the overall hydrogen concentration in the solid by transfer of hydrogen across the external surfaces of the solid. Such a system in which local equilibration can be achieved without any exchange of hydrogen with the system's thermodynamic reservoir is termed "closed" (Sofronis and Birnbaum, 1995).

Symmetry permits the analysis to be confined to a semi-circular domain as shown in Fig. 1 with the crack lying along $x_1 < 0$. The crack surface is traction free and the symmetry line is free of shear traction and displacement normal to the line.

FINITE ELEMENT CALCULATIONS

The finite element method was used to solve the boundary value problem as stated in the previous section. Letting $\{q\}$ denote the array of nodal displacements and using the standard interpolation matrices, **[A]** for the displacement, **[B]** for the strain and **[C]** for the constitutive law of an isotropic material, one can rewrite the governing eqn (11) as follows:

$$[\mathbf{K}]\{q\} = \{F\} + \{F'\}, \tag{12}$$

where

$$[\mathbf{K}] = \int_A [\mathbf{B}]^T[\mathbf{C}][\mathbf{B}]\,\mathrm{d}A, \tag{13}$$

$$\{F\} = \int_S [\mathbf{A}]^T\{T\}\,\mathrm{d}S, \tag{14}$$

$$\{F'\} = \int_A [\mathbf{B}]^T[\mathbf{C}]\{\varepsilon^h\}\,\mathrm{d}A \tag{15}$$

$$\{\varepsilon^h\}^T = [\varepsilon_{11}^H \;\; \varepsilon_{22}^H \;\; \varepsilon_{33}^H \;\; 0], \tag{16}$$

and the superscript T stands for array or matrix transpose. The iterative procedure to solve eqns (12)–(16) is described in the work by Sofronis and Birnbaum (1993).

The finite element discretization divided the domain (see Fig. 1) into 18 equal angular zones and 100 geometrically scaled radial zones. The geometric scaling of the radial length allows for fine near tip discretization in order to ensure that the zone of large hydrogen concentrations is determined fairly reliably. The distance from the crack tip to the outer boundary was set to equal 7.93 cm, although half of the elements were within 25 microns from the crack tip. Thus the mesh consisted of 1782 four-noded isoparametric equilateral rectangles and 18 four-noded isoparametric degenerate isosceles triangles, with a total of 1901 nodes. Four integration stations were used in each element to integrate the stiffness. The local hydrogen concentrations were evaluated at the elemental centroids through an averaged hydrostatic stress.

The stiffness derivative method (Parks, 1974) was used to determine the local stress intensity factor at the crack tip, K_I, which describes the crack tip fields in a linear elastic material. Because the transformation strain due to solute hydrogen is purely dilatational (Peisl, 1978) and hence it is solely a function of hydrostatic stress the solid solution material is hyperelastic (McMeeking and Evans, 1982; Budiansky *et al.*, 1982). The complementary energy density, $\psi(\sigma)$, is calculated by

$$\psi = \int_0^{\sigma_{ij}} \varepsilon_{ij}\,\mathrm{d}\sigma'_{ij}. \tag{17}$$

Introducing the strain energy density $w = \sigma_{ij}\varepsilon_{ij} - \psi$, one can define the potential energy of the system

$$\Pi = \int_A w\,\mathrm{d}A - \int_{S_T} T_i u_i\,\mathrm{d}S, \tag{18}$$

where S_T is the portion of the boundary S where tractions are prescribed. The energy release rate, G, is then calculated from the change in the potential energy due to a virtual crack extension Δx along the x_1-axis (see Fig. 1) as

$$G = -\frac{\partial \Pi}{\partial x}. \tag{19}$$

Combining eqns (18) and (19), equilibrium eqns (12), and the zero traction condition along the crack faces, one by using hyperelasticity, $\sigma_{ij} = \partial w/\partial \varepsilon_{ij}$, can derive the finite element form for the energy release rate

$$G = -\int_A \{q\}^T \frac{\partial [\mathbf{B}]}{\partial x}\{\sigma\}\,\mathrm{d}A, \tag{20}$$

where $\{q\}$ and $\{\sigma\}$ denote solution arrays for the nodal displacements and stresses respectively. Numerical values for $\partial[\mathbf{B}]/\partial x$ were obtained through forward Euler differencing, i.e. $\partial[\mathbf{B}]/\partial x = ([\mathbf{B}]_{x+\Delta x} - [\mathbf{B}]_x)/\Delta x$. Values of Δx equal to 10^{-6} the typical elemental dimension were found to provide excellent values for G (Parks, 1977). The local stress intensity factor at the tip, K_I, was calculated from the relation

$$G = \frac{1-\nu^2}{E} K_I^2, \tag{21}$$

where E and ν are respectively the Young's modulus and Poisson's ratio.

RESULTS

Finite element solutions were obtained for the niobium system at loads, K_A, equal to 20, 40, 60, 80 and 100 MPa$\sqrt{\text{m}}$; and nominal concentrations of $H/M = 10^{-6}$, 10^{-5}, 10^{-4}, 0.001, 0.01 and 0.1. The system's temperature was 300 K and eqn (6) for the hydrogen lattice dilatation had the form $e^H = 0.174c$ (Peisl, 1978). For each combination of load and nominal concentration two sets of calculations were made, one set using the hydrogen free material moduli and another set using the hydrogen dependent moduli as dictated by eqns (8) and (9).

In the case when the hydrogen effect on the constitutive moduli was not accounted for, the stress fields near the crack tip were found independent of the nominal hydrogen concentration c_0. In Fig. 2 the normalized stress σ_{22}/E_0, where parameter E_0 is the Young's modulus of the hydrogen free material, is shown plotted against normalized distance $r/(K_A/E_0)^2$ from the crack tip at $\theta = 0$; applied loads of $K_A = 20$, 60 and 100 MPa$\sqrt{\text{m}}$; and for any nominal concentration c_0. In particular, the near tip stress fields were found to be identical to those of the hydrogen free material regardless of the value of c_0. This situation is shown in Fig. 3 where the normalized stress σ_{22}/E_0 is plotted against distance r from the crack tip at $\theta = 0$; load $K_A = 100$ MPa$\sqrt{\text{m}}$; and nominal concentrations of $H/M = 0$, 10^{-6}, 0.001 and 0.1. It should be noted that the magnitude of the stress in Figs 2 and 3 is of the order of Young's modulus because the calculations were carried out on the assumption that the material does not yield plastically. As will be shown, the absence of any hydrogen effect on the near tip stresses is an expected result in view of the hyperelastic nature of the material and the path independence of the J-Integral (Rice, 1968a; McMeeking and Evans, 1982; Budiansky *et al.*, 1982).

When the modulus change was considered, the hydrogen effect on the near tip stresses was independent of the nominal hydrogen concentration because the local hydrogen distribution immediately ahead of the crack tip was found to be the same for any nominal concentration. In all cases the presence of hydrogen caused the near tip stresses to be reduced in comparison to those in the hydrogen free material. The hydrogen modulus effect

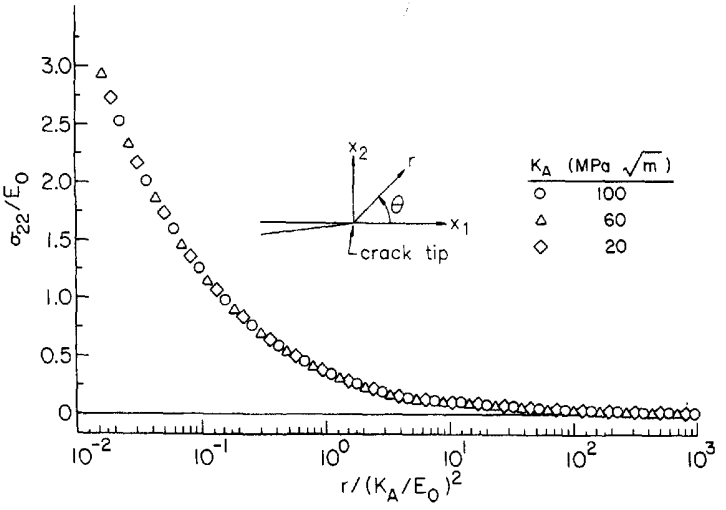

Fig. 2. Plot of normalized stress σ_{22}/E_0 vs normalized distance $r/(K_A/E_0)^2$ ahead of the crack tip at $\theta = 0$; applied loads of $K_A = 20$, 60 and 100 MPa$\sqrt{\text{m}}$; and for any nominal concentration c_0. Parameter K_A is the applied stress intensity factor and E_0 is the Young's modulus. The hydrogen effect on the elastic moduli was not accounted for.

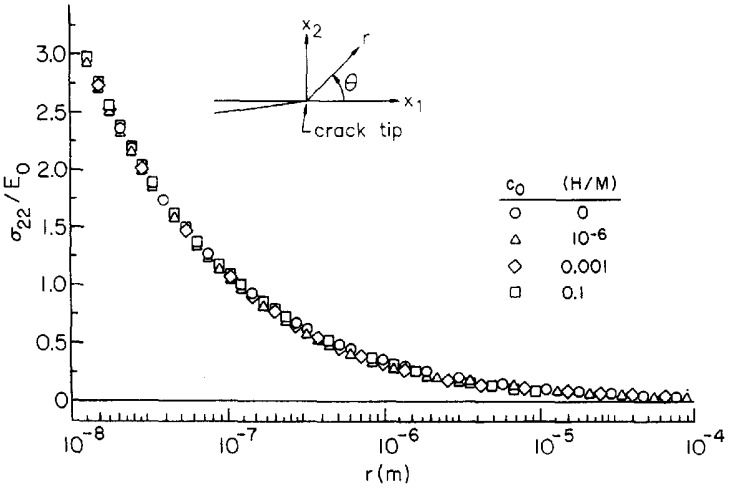

Fig. 3. Plot of normalized stress σ_{22}/E_0 vs distance r ahead of the crack tip at $\theta = 0$; load $K_A = 100\,\text{MPa}\sqrt{\text{m}}$; and nominal concentrations of $H/M = 0$, 10^{-6}, 0.001 and 0.1. The hydrogen effect on the elastic moduli was not accounted for.

at $K_A = 100\ \text{MPa}\sqrt{\text{m}}$ is shown in Fig. 4 where the normalized stress σ_{22}/E_0 is plotted against distance r from the crack tip at $\theta = 0$ and nominal concentrations of $H/M = 0$, 10^{-6}, 0.001 and 0.1. The reduction of the stress ahead of the crack tip is a result of the hydrogen induced material modulus softening (cf. eqn (8)).

In all calculations a zone of hydrogen saturated material can be found in the vicinity of the crack tip (see Fig. 5). A zone is described to be saturated with hydrogen when the local hydrogen concentration H/M is 99.5% of the lattice saturation concentration which is equal to 1. The existence of the zone is a consequence of the Fermi-Dirac statistics used in calculating the hydrogen concentrations combined with the singular nature of the stress at the crack tip. The size of the hydrogen saturated zone is clearly a function of the nominal hydrogen concentration and the applied load. Figure 6 shows the hydrogen concentration H/M ahead of the crack tip at $\theta = 0$ plotted against distance r from the crack tip at load levels of $K_A = 20$, 60, and $100\ \text{MPa}\sqrt{\text{m}}$, and for fixed nominal concentration $H/M = 10^{-6}$. A similar concentration profile is shown in Fig. 7 under a constant load of $100\ \text{MPa}\sqrt{\text{m}}$ and nominal concentrations of $H/M = 10^{-6}$, 0.001, and 0.1. These results are summarized in Fig. 8 where the hydrogen concentration H/M ahead of the crack tip at $\theta = 0$ is plotted

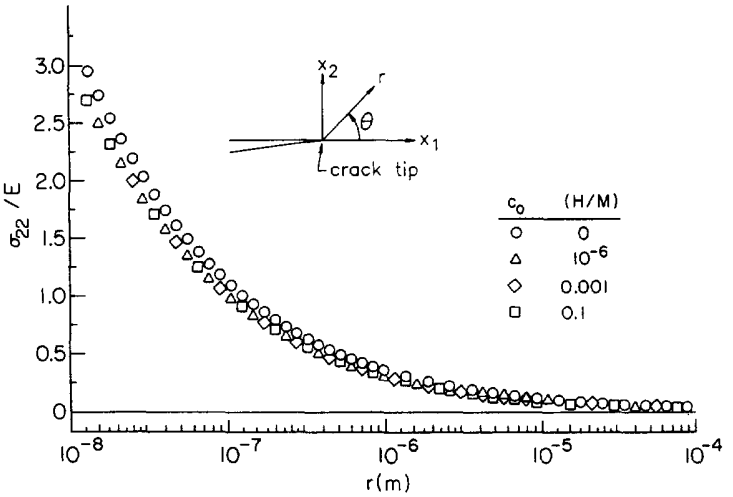

Fig. 4. Plot of normalized stress σ_{22}/E_0 vs distance r ahead of the crack tip at $\theta = 0$, load $K_A = 100\,\text{MPa}\sqrt{\text{m}}$, and nominal concentrations of $H/M = 0$, 10^{-6}, 0.001 and 0.1. The hydrogen effect on the elastic moduli was accounted for.

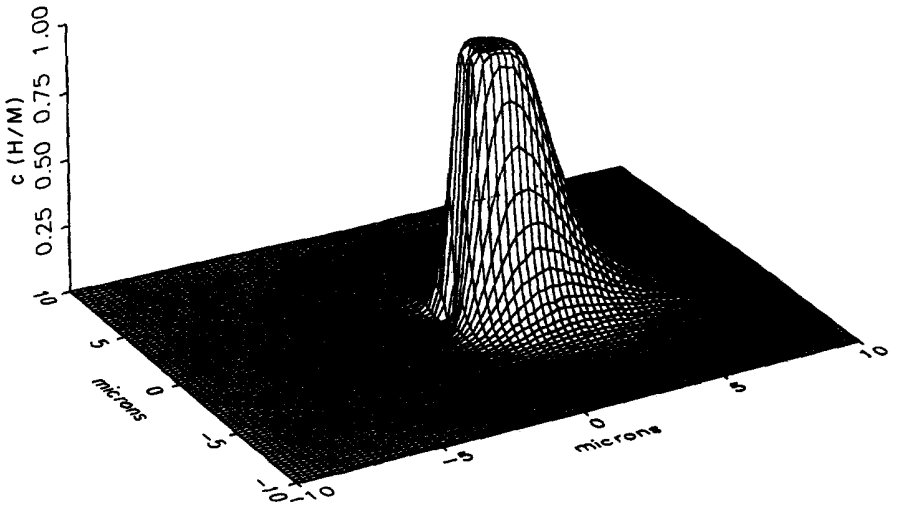

Fig. 5. Surface plot of hydrogen concentration in H/M around a crack tip at load $K_A = 100\,\text{MPa}\sqrt{\text{m}}$ and nominal concentration $c_0 = 10^{-6}$. The hydrogen effect on the elastic moduli was accounted for.

vs normalized distance $r/(K_A/E_0)^2$ from the tip at nominal concentrations of $H/M = 10^{-6}$, 0.001, and 0.1, and for any level of applied load. Figure 8 demonstrates that the hydrogen distribution ahead of the crack tip scales directly with the applied loads. This is an expected result because local concentrations are always in equilibrium with the corresponding stresses. In Fig. 9 the saturation zone size, r_s, ahead of the crack tip at $\theta = 0$ is plotted against nominal concentration c_0 under load levels of $K_A = 20$, 40, 60, 80 and 100 $\text{MPa}\sqrt{\text{m}}$. For the same applied loads the corresponding normalized saturation zone size $r_s/(K_A/E_0)^2$ is plotted in Fig. 10 against nominal concentration c_0. Figure 10 clearly demonstrates that the normalized saturation zone size $r_s/(K_A/E_0)^2$ depends only on the nominal hydrogen concentration alone and not on the applied loads, the result thus being in accord with Fig. 8.

Stress intensity factors were calculated by computing the integral of eqn (20) with the use of a ring of elements (Parks, 1974) surrounding the crack tip well within the saturation zone. If one considers the path independence of the J-integral

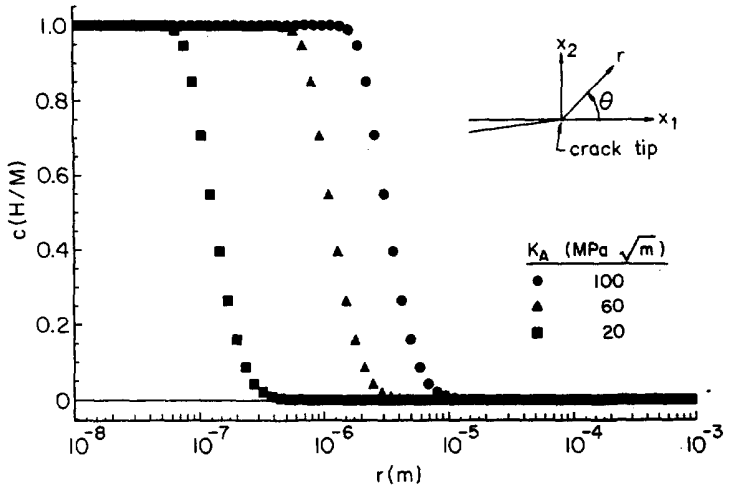

Fig. 6. Plot of hydrogen concentration c ahead of the crack tip at $\theta = 0$ vs distance r from the tip at nominal concentration $c_0 = 10^{-6}$ and applied loads of $K_A = 20$, 60 and 100 $\text{MPa}\sqrt{\text{m}}$. The hydrogen effect on the elastic moduli was accounted for.

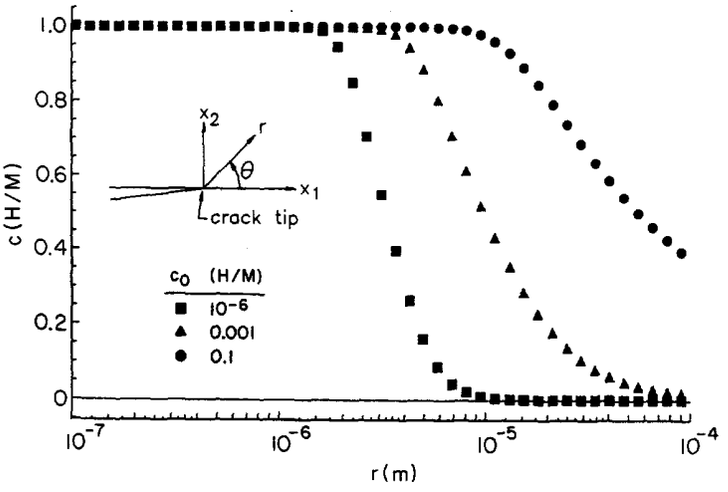

Fig. 7. Plot of hydrogen concentration c ahead of the crack tip at $\theta = 0$ vs distance r from the tip at applied load of $K_A = 100\,\text{MPa}\sqrt{\text{m}}$ and nominal concentrations of $H/M = 10^{-6}$, 0.001 and 0.1. The hydrogen effect on the elastic moduli was accounted for.

$$\frac{1-\nu_t^2}{E_t}K_t^2 = \frac{1-\nu_0^2}{E_0}K_A^2, \tag{22}$$

where E_t, ν_t are the moduli within the saturation zone calculated from eqns (8) and (9) for $c = 1$, and E_0, ν_0 are those for the hydrogen free material, $c = 0$. Obviously, in the absence of the modulus effect $E = E_0$, $\nu = \nu_0$ and eqn (22) implies $K_t = K_A$. This result confirms the numerical calculations presented in Fig. 2 which shows that there is no hydrogen effect on the near tip stresses, when the modulus effect is not considered. However, when the modulus effect is accounted for, the local crack tip stress intensity factor, K_t, was found independent of both levels of nominal concentration and applied load and it was equal to 0.9 K_A in all cases. This 10% reduction of the load intensity scales directly with the hydrogen induced modulus softening inside the saturation zone and correlates well with the reduction in near tip stresses shown in Fig. 4.

DISCUSSION

Due to the singular nature of the stress field in the elastic solution the model predicts that a zone of hydrogen saturated material always forms near the crack tip after a period

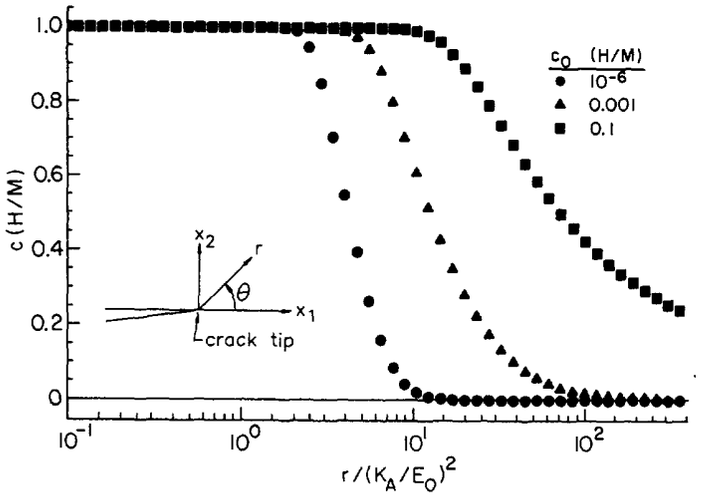

Fig. 8. Plot of hydrogen concentration c ahead of the crack tip at $\theta = 0$ vs normalized distance $r/(K_A/E_0)^2$ from the tip at nominal concentrations of $H/M = 10^{-6}$, 0.001 and 0.1, and for any level of applied load. The hydrogen effect on the elastic moduli was accounted for.

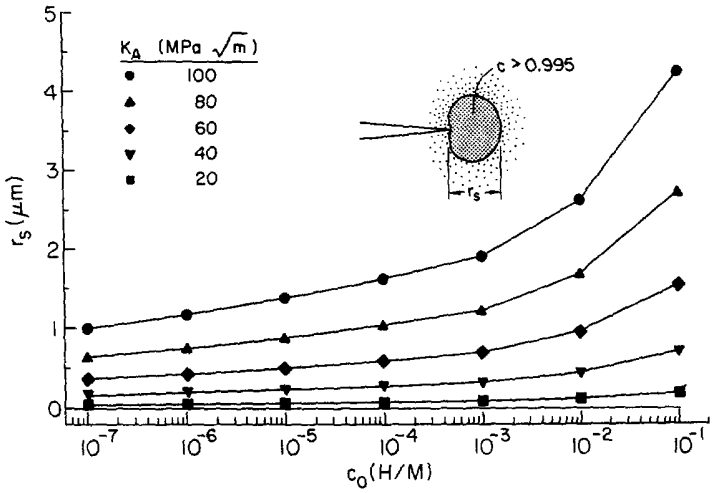

Fig. 9. Plot of the saturation zone size, r_s, ahead of the crack tip at $\theta = 0$ against nominal concentration c_0 at loads of $K_A = 20$, 40, 60, 80 and 100 MPa$\sqrt{m}$. The hydrogen effect on the elastic moduli was accounted for.

of hydrogen diffusion which is much greater than the characteristic diffusion time for the system. Inside the saturation zone the hydrogen concentration gradients are essentially equal to zero (see Fig. 8) and consequently the local hydrogen induced dilatational strain and local isotropic elastic moduli are uniform. In general, the saturation zone size increases monotonically with increasing nominal concentration and applied load. At nominal concentrations of H/M less than 0.001 and applied loads of intensity less than approximately 60 MPa$\sqrt{m}$ the saturation zone size, r_s, is almost independent of the nominal concentration and it is essentially the applied loads which determine the magnitude of the zone (see Fig. 9). However, at nominal concentrations larger than 0.001 the zone size increases markedly with increasing values of nominal concentrations. At nominal concentrations less than 0.1 and applied loads less than 100 MPa$\sqrt{m}$ (see Fig. 9) the zone size ahead of the crack tip does not exceed about 4μm. For the same range of nominal concentrations and external loads the normalized zone size, which is independent of the applied loads, is always less than 6 (see Fig. 10).

The hydrogen saturated zone, which for a wide range of loads spans the region within a radius less than 4μm ahead of the crack tip, is sufficiently large to allow for a continuum

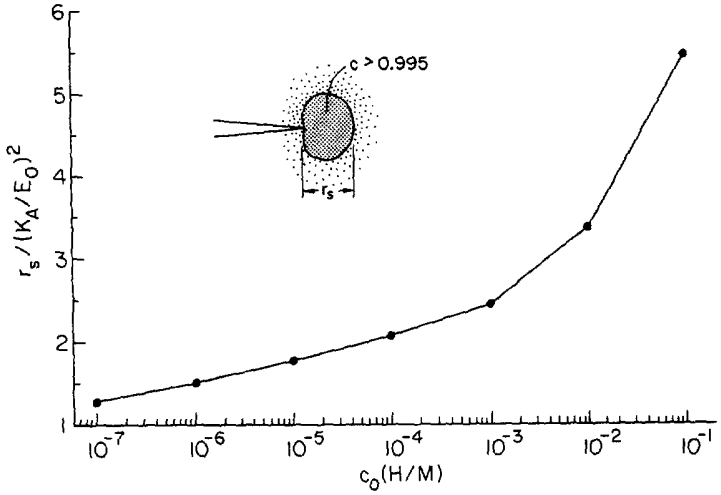

Fig. 10. Plot of the normalized saturation zone size, $r_s/(K_A/E_0)^2$, ahead of the crack tip at $\theta = 0$ against nominal concentration c_0 at loads of $K_A = 20$, 40, 60, 80 and 100 MPa$\sqrt{m}$. The hydrogen effect on the elastic moduli was accounted for.

description of the hydrogen induced volume and modulus change effects on the lattice. As a result, within the model assumptions, the existence of this hydrogen saturated zone of material can affect the crack tip stress field and in turn, the fracture resistance of the material. The near tip stress singular elastic solution is characterized by the local stress intensity factor, K_t, which is lower than the applied load intensity, K_A, due to hydrogen induced softening of the elastic moduli.

Local stresses outside the K_t dominance region are affected by the hydrogen concentration gradients which exist between the inner saturated zone and the outer region with nominal hydrogen concentration. Since the absolute size of the saturation zone is a function of the applied load and the nominal hydrogen concentration, the location of these hydrogen concentration gradients relative to the crack tip varies accordingly. However, since the singular elastic solution always leads to a saturated zone regardless of the size of the applied load and nominal hydrogen concentration, the near tip stresses are solely characterized by the local stress intensity factor, K_t, determined by eqn (22) and not by the hydrogen concentration gradients.

The magnitude of the calculated stresses inside the saturation zone has been found to be of the order of Young's modulus of the material in view of the elasticity assumption. In Fig. 4 the stress σ_{22} ahead of the crack tip inside the saturation zone is always greater than $0.2E_0$. Evidently, such stresses are too large for a material to sustain without plastic yielding. The hydrostatic stresses required to saturate the lattice with solute hydrogen, $c = 0.995$, can be calculated using eqn (3). Representative values of $\sigma_{kk}/3$ are given in Table 1 as a function of nominal concentration c_0 for the niobium and single crystal Fe-3wt. %Si systems. The partial molar volume of hydrogen in solution with Fe was taken as 2 cm^3/mole (Hirth, 1980). For both systems the hydrostatic stress required for the lattice to saturate is approximately 25GPa and 15GPa for nominal concentrations of $H/M = 10^{-6}$ and 0.001 respectively. However, if plastic straining is present and the crack tip blunts open the plastic incompressibility constraint limits the magnitude of the hydrostatic stress to approximately 1.2GPa (McMeeking, 1977) when the yield stress of the material is taken 300 MPa. Therefore for typical metals and alloys the maximum hydrogen concentration would be significantly less than saturation levels predicted in the present paper.

The insufficiency of elasticity alone to model the hydrogen effects at a crack tip becomes clearer if one considers the typical length scales associated with plastic deformation. In the absence of hydrogen, it is well established (McMeeking, 1977; Hutchinson, 1983) that ahead of a blunting crack tip there exists a fracture process zone in which the material undergoes intense plastic straining (see Fig. 11). The typical length of this zone (see Fig. 11) is $3\delta_t$, where δ_t is the crack tip opening displacement calculated from $\delta_t = 0.6(1-\nu^2)(\sigma_0/E)(K_A/\sigma_0)^2$ (McMeeking, 1977) and σ_0 is the yield stress. Considering $K_A = 20\,\text{MPa}\sqrt{\text{m}}$, which is a relatively low level of applied load, one finds the size of the fracture process zone, r_{pr}, to be for typical cases as follows: (a) 13.4 μm for niobium of low yield stress, $\sigma_0 = 100$ MPa, with $E = 114$ GPa and $\nu = 0.38$; (b) 2.6 μm for high strength steels with $\sigma_0 = 1200$ MPa, $E = 207$ GPa, and $\nu = 0.3$; (c) 16.5 μm for Fe-3wt. %Si with $\sigma_0 = 300$ MPa, $E = 132$ GPa, and $\nu = 0.3$ (Chen *et al.*, 1990). The present elastic calculations which are pertinent to the niobium system predict a hydrogen saturation zone size less than 4 μm for a wide range of loads. Therefore, for typical metals and alloys, one may

Table 1. Hydrostatic stress, $\sigma_{kk}/3$, in GPa, required for lattice saturation, i.e. $c = 0.995$, vs nominal hydrogen concentration c_0

c_0 (H/M)	Niobium	Iron
10^{-6}	25.3	24.3
10^{-5}	22.3	21.3
10^{-4}	19.2	18.4
10^{-3}	16.2	15.5
10^{-2}	13.1	12.6
10^{-1}	9.9	9.5

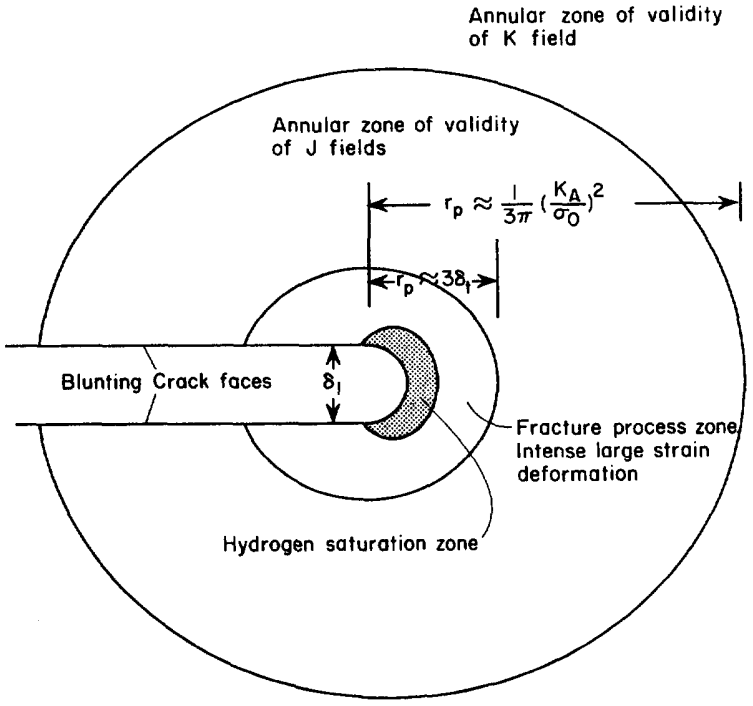

Fig. 11. Schematic description of the elastic-plastic deformation at a blunting crack tip in the absence of hydrogen with superposed hydrogen saturation zone obtained via elastic analysis.

infer that the hydrogen saturated zone lies inside the process zone which is characterized by intense plastic straining. Consequently, elasticity alone can only be used to model hydrogen effects on materials of extremely high yield strength under load levels of just a few MPa$\sqrt{m}$ when phrased in terms of the applied stress intensity factors. If the material is capable of yielding plastically the hydrogen distribution at a crack tip and its associated effects on fracture toughness should be sought through a large strain elastic-plastic analysis as in the work by Sofronis and McMeeking (1989). That work though, despite its detailed analysis of transient hydrogen diffusion coupled with elastic-plastic straining at a blunting crack is phenomenological too, and it does not incorporate any possible mechanisms for hydrogen induced failure, either.

In the cases when the elasticity assumption is valid, continuum mechanics calculations predict that hydrogen induced softening of the elastic moduli results in crack tip shielding from the applied loads. In addition, due to the high mobility of hydrogen it is highly unlikely that any transient effects might result in types of straining at the tip markedly different from those modeled in the present paper. Therefore one could use the present analysis to discuss the hydrogen embrittlement phenomenon in conjunction with the hydrogen intrinsic effects, in case they were known, on the critical stress intensity factor, K_{IC}, for crack propagation. For instance, the reduction of the surface energy is pertinent to the decohesion mechanism of hydrogen embrittlement but the main difficulty in this theory lies in relating the surface energy or other physical parameters (Birnbaum, 1979) to the fracture stress and the local hydrogen concentration. Hence, the present discussion is limited only to mechanistic phenomena related to the hydrogen presence at a crack tip. In general, hydrogen embrittlement requires crack tip anti-shielding which can only happen, within the context of the present analysis, in a system whose moduli are stiffened by hydrogen. If modulus softening is the case, as in niobium, then for anti-shielding to be observed preferential hydrogen accumulation directly ahead of the crack tip is required (McMeeking and Evans, 1982). Hence, it seems that the present elastic model should be extended to include the effects of the microstructure, such as background dislocations at the crack tip. Such a treatment, on one hand, accounts for plastic straining of the material and thereby elimination of the enormously large stresses ahead of the crack tip; and on the other hand,

it allows for regions of localized hydrogen distributions possibly tied with crack tip anti-shielding phenomena (Hirsch *et al.*, 1992).

CLOSURE

The hydrogen induced volume dilatation and modulus softening was investigated in the vicinity of a crack tip in the niobium system which was modeled as linearly elastic and isotropic. Hydrogen solute concentrations were assumed to be in equilibrium with local stresses and the hydrogen distribution was calculated by Fermi-Dirac statistics which allows for interstitial lattice site saturation. Stresses in the material were calculated by accounting for the hydrogen induced local volume relaxation due to the associated dilatational strain and local modulus change. The numerical results showed that a zone of hydrogen saturated lattice is found ahead of the crack tip. The size of this zone depends on the applied loads and the nominal hydrogen concentration. A non-dimensionalized length of the hydrogen saturated zone can be defined which is found to be independent of the applied load. This result is in accord with the model assumption of hydrogen equilibration with local stresses. Calculations of the local crack tip stress intensity factor reproduce the well known result that if the modulus effect is not accounted for, there is no change in the intensity of the applied loads transmitted to the crack tip. However, when the effects of hydrogen on the moduli were included, crack tip shielding was observed. The magnitude of shielding, when measured in terms of the decrease in the applied stress intensity factor, scales with the amount of modulus reduction inside the saturation zone and is independent of both nominal hydrogen concentration and level of applied loads. Comparison of the hydrogen saturation zone size with the size of the elastic-plastic fracture process zone in typical metals and alloys indicates the need for plasticity considerations in the study of the hydrogen interactions with a crack tip under load.

Acknowledgments—The authors would like to thank professor H. K. Birnbaum for many helpful discussions and comments on this paper. This work was supported by the Department of Energy under grant DEFGO2-91ER45439.

REFERENCES

Birnbaum, H. K. (1979). Hydrogen related failure mechanisms in metals. In *Environmental Sensitive Fracture of Engineering Materials* (Proceedings of Symposium on Environmental Effects on Fracture, Chicago, Illinois, October 24–26, 1977) (ed. Z. A. Foroulis), pp. 326–360. Metallurgical Society of AIME, Warendale, Pennsylvania.

Birnbaum, H. K. and Sofronis, P. (1994). Hydrogen-enhanced localized plasticity—a mechanism for hydrogen-related fracture. *Mat. Sci. Engng* **A176,** 191–202.

Budiansky, B., Hutchinson, J. W. and Lambropoulos, J. C. (1983). Continuum theory of dilatant transformation toughening in ceramics. *Int. J. Solids Structures* **19,** 337–355.

Chen, X., Foecke, T., Lii, M., Katz, Y. and Gerberich, W. W. (1990). The role of stress state on hydrogen cracking in Fe-Si single crystals. *Engng Fract. Mech.* **35,** 997–1017.

Cottrell, A. H. (1948). Effects of solute atoms on the behaviour of dislocations. In *Report of a conference on Strength of Solids*, H. H. Wills Physical Laboratory, University of Bristol, 7–9 July 1947, pp. 30–36. The Physical Society, London.

Dutton, R., Nuttall, K., Puls, M. P. and Simpson, L. A. (1977). Mechanisms of hydrogen induced delayed cracking in hydride forming materials. *Met. Trans.* **8A,** 1553–1562.

Eshelby, J. D. (1956). The continuum theory of lattice defects. In *Solid State Physics* (eds F. Seitz and D. Turnbull), Vol. 3, pp. 79–144. Academic Press, New York.

Eshelby, J. D. (1957). The determination of the elastic field of an ellipsoidal inclusion and related problems. *Proc. R. Soc.* **A241,** 376–396.

Hippsley, C. A. and Briant, C. L. (1985). Application of a model for stress driven segregation to hydrogen embrittlement. *Scr. Met.* **19,** 1203–1208.

Hirsch, P., B., Booth, A. S., Ellis, M. and Roberts, S. G. (1992). Dislocation-driven stable crack growth by microcleavage in semi-brittle crystals. *Scr. Met.* **27,** 1723–1728.

Hirth, J. P. (1980). Effects of hydrogen on the properties of iron and steel. *Met Trans.* **11A,** 861–890.

Hirth, J. P. and Carnahan, B. (1978). Hydrogen adsorption at dislocations and cracks in Fe. *Acta Metall.* **26,** 1795–1803.

Hutchinson, J. W. (1983). Fundamentals of the phenomenological theory of nonlinear fracture mechanics. *J. Appl. Mech.* **50,** 1042–1051.

Irwin, G. R. (1960). Fracture Mechanics. In *Structural Mechanics* (Proceedings of the First Symposium of Naval Structural Mechanics) (ed. J. N. Goodier and N. J. Hoff), pp. 557–594. Stanford University, August 1958.

Liu, H. W. (1970). Stress-corrosion cracking and the interaction between crack-tip stress field and solute atoms. *J. Bas. Engng, Trans. ASME* **92,** 633–638.

Mazzolai, F. M. and Birnbaum, H. K. (1985a). Elastic constants and ultrasonic attenuation of the $\alpha-\alpha'$ phase of the Nb-H(D) system. I: Results. *J. Phys. F: Met. Phys.* **15,** 507–523.

Mazzolai, F. M. and Birnbaum, H. K. (1985b). Elastic constants and ultrasonic attenuation of the $\alpha-\alpha'$ phase of the Nb-H(D) system. II: Interpretation of results. *J. Phys. F: Met. Phys.* **15,** 525–542.

McMeeking, R. M. (1977). Finite deformation analysis of crack-tip opening in elastic-plastic materials and implications for fracture. *J. Mech. Phys. Solids* **25,** 357–381.

McMeeking, R. M. and Evans, A. G. (1982). Mechanics of transformation-toughening in brittle materials. *J. Am. Ceram. Soc.* **65,** 242–246.

Parks, D. M. (1974). A Stiffness derivative finite element technique for determination of crack tip stress intensity factors. *Int. J. Fract. Mech.* **10,** 487–502.

Parks, D. M. (1977). The virtual crack extension method for nonlinear material Behavior. *Comp. Meth. Appl. Mech. Engng* **12,** 353–364.

Peisl, H. (1978). Lattice strains due to hydrogen in metals. In *Hydrogen in Metals I, Topics in Applied Physics* (ed. G. Alefeld and J. Volkl), Vol. 28, pp. 53–74. Springer-Verlag, New York.

Rice, J. R. (1968a). A path independent integral and the approximate analysis of strain concentration by notches and cracks. *J. Appl. Mech.* **35,** 379–386.

Rice, J. R. (1968b). Mathematical analysis in the mechanics of fracture. In *Fracture: An Advanced Treatise* (ed. H. Liebowitz), Vol. 12, pp. 191–311. Academic Press, New York.

Sofronis, P. and Birnbaum, H. K. (1993). Mechanics of hydrogen-dislocation-impurity interactions: part I-increasing shear modulus. *TAM Report No.* 729, *UILU-ENG*-93-6027, University of Illinois at Urbana-Champaign, Urbana, Illinois.

Sofronis, P. and Birnbaum, H. K. (1995). Mechanics of the hydrogen-dislocation-impurity interactions: part I—increasing shear modulus. *J. Mech. Phys. Solids* **43,** 49–90.

Sofronis, P. and McMeeking, R. M. (1989). Numerical analysis of hydrogen transport near a blunting crack tip. *J. Mech. Phys. Solids* **37,** 317–350.

Tong-Yi, Z., Mason, T. A. and Hack, J. E. (1992a). The equilibrium concentration of hydrogen atoms ahead of a mode I crack tip single crystal iron. *Scr. Met.* **26,** 139–144.

Tong-Yi, Z., Shen, H. and Hack, J. E. (1992b). The influence of cohesive forces on the equilibrium concentration of hydrogen atoms ahead of a crack tip in single crystal iron. *Scr. Met.* **27,** 1605–1610.

Unger, D. J. (1989). A mathematical analysis for impending hydrogen assisted crack propagation. *Engng Fract. Mech.* **34,** 657–667.

Van Leeuwen, H. P. (1974). The kinetics of hydrogen embrittlement: a quantitative diffusion model. *Engng Fract. Mech.* **6,** 141–161.

Weertman, J. and Hack, J. E. (1988). Crack tip shielding/antishielding by impurity atoms. *Int. J. Fract. Mech.* **36,** 27–34.